



LABORATORI NAZIONALI DI FRASCATI  
SIS-Pubblicazioni

**LNF-02/004(P)**

22 Aprile 2002

hep-ex/0204024

**Measurement of  $\Gamma(K_S \rightarrow \pi^+\pi^-(\gamma))/\Gamma(K_S \rightarrow \pi^0\pi^0)$**

The KLOE Collaboration\*

**Abstract**

We have measured the ratio  $R_S^\pi = \Gamma(K_S \rightarrow \pi^+\pi^-(\gamma))/\Gamma(K_S \rightarrow \pi^0\pi^0)$  with the KLOE detector at the DAΦNE  $e^+e^-$  collider. This measurement is fully inclusive with respect to the  $\pi^+\pi^-\gamma$  final state. The sample of over  $10^6$  two-pion decays of tagged  $K_S$  mesons allows a statistical error as low as  $\sim 0.1\%$  to be obtained. The accuracy is limited by systematic uncertainties, which are estimated primarily from data. We find  $R_S^\pi = 2.236 \pm 0.003_{\text{stat}} \pm 0.015_{\text{sys}}$ .

PACS:13.20.Eb

Submitted to Elsevier Science for publication on Phys. Lett. B.

## \* The KLOE Collaboration

A. Aloisio<sup>b</sup>, F. Ambrosino<sup>b</sup>, A. Antonelli<sup>d</sup>, M. Antonelli<sup>d</sup>, C. Bacci<sup>e</sup>, R. Baldini-Ferroli<sup>d</sup>,  
G. Bencivenni<sup>d</sup>, S. Bertolucci<sup>d</sup>, C. Bini<sup>g</sup>, C. Bloise<sup>d</sup>, V. Bocci<sup>g</sup>, F. Bossi<sup>d</sup>, P. Branchini<sup>e</sup>,  
S. A. Bulychjov<sup>c</sup>, G. Cabibbo<sup>g</sup>, R. Caloi<sup>g</sup>, P. Campana<sup>d</sup>, G. Capon<sup>d</sup>, G. Carboni<sup>a</sup>,  
M. Casarsa<sup>f</sup>, V. Casavola<sup>h</sup>, G. Cataldi<sup>h</sup>, F. Ceradini<sup>e</sup>, F. Cervelli<sup>i</sup>, F. Cevenini<sup>b</sup>,  
G. Chiefari<sup>b</sup>, P. Ciambrone<sup>d</sup>, S. Conetti<sup>o</sup>, E. De Lucia<sup>g</sup>, G. De Robertis<sup>j</sup>, P. De Simone<sup>d</sup>,  
G. De Zorzi<sup>g</sup>, S. Dell'Agello<sup>d</sup>, A. Denig<sup>d</sup>, A. Di Domenico<sup>g</sup>, C. Di Donato<sup>b</sup>,  
S. Di Falco<sup>m</sup>, A. Doria<sup>b</sup>, M. Dreucci<sup>d</sup>, O. Erriquez<sup>j</sup>, A. Farilla<sup>e</sup>, G. Felici<sup>d</sup>, A. Ferrari<sup>e</sup>,  
M. L. Ferrer<sup>d</sup>, G. Finocchiaro<sup>d</sup>, C. Forti<sup>h</sup>, A. Franceschi<sup>d</sup>, P. Franzini<sup>g</sup>, C. Gatti<sup>i</sup>,  
P. Gauzzi<sup>g</sup>, S. Giovannella<sup>d</sup>, E. Gorini<sup>h</sup>, F. Grancagnolo<sup>h</sup>, E. Graziani<sup>e</sup>, S. W. Han<sup>d,k</sup>,  
M. Incagli<sup>i</sup>, L. Ingrosso<sup>d</sup>, W. Kluge<sup>m</sup>, C. Kuo<sup>m</sup>, V. Kulikov<sup>c</sup>, F. Lacava<sup>g</sup>, G. Lanfranchi<sup>d</sup>,  
J. Lee-Franzini<sup>d,l</sup>, D. Leone<sup>g</sup>, F. Lu<sup>d,k</sup>, M. Martemianov<sup>m</sup>, M. Matsyuk<sup>d,c</sup>, W. Mei<sup>d</sup>,  
L. Merola<sup>b</sup>, R. Messi<sup>a</sup>, S. Miscetti<sup>d</sup>, M. Moulson<sup>d</sup>, S. Müller<sup>m</sup>, F. Murtas<sup>d</sup>,  
M. Napolitano<sup>b</sup>, A. Nedosekin<sup>d,c</sup>, F. Nguyen<sup>e</sup>, M. Palutan<sup>a</sup>, L. Paoluzi<sup>a</sup>, E. Pasqualucci<sup>g</sup>,  
L. Passalacqua<sup>d</sup>, A. Passeri<sup>e</sup>, V. Patera<sup>n,d</sup>, E. Petrolo<sup>g</sup>, G. Pirozzi<sup>b</sup>, L. Pontecorvo<sup>g</sup>,  
M. Primavera<sup>h</sup>, F. Ruggieri<sup>j</sup>, P. Santangelo<sup>d</sup>, E. Santovetti<sup>a</sup>, G. Saracino<sup>b</sup>,  
R. D. Schamberger<sup>l</sup>, B. Sciascia<sup>d</sup>, A. Sciubba<sup>n,d</sup>, F. Scuri<sup>f</sup>, I. Sfligoj<sup>d</sup>, T. Spadaro<sup>d</sup>,  
E. Spiriti<sup>e</sup>, G. L. Tong<sup>d,k</sup>, L. Tortora<sup>e</sup>, E. Valente<sup>g</sup>, P. Valente<sup>d</sup>, B. Valeriani<sup>m</sup>,  
G. Venanzoni<sup>i</sup>, S. Veneziano<sup>g</sup>, A. Ventura<sup>h</sup>, Y. Xu<sup>d,k</sup>, Y. Yu<sup>d,k</sup>

<sup>a</sup> Dipartimento di Fisica dell'Università "Tor Vergata" e Sezione INFN, Roma, Italy

<sup>b</sup> Dipartimento di Scienze Fisiche dell'Università "Federico Secondo" e Sezione INFN,  
Napoli, Italy

<sup>c</sup> Permanent address: Institute for Theoretical and Experimental Physics, Moscow,  
Russia

<sup>d</sup> Laboratori Nazionali di Frascati dell'INFN, Frascati, Italy

<sup>e</sup> Dipartimento di Fisica dell'Università "Roma Tre" e Sezione INFN, Roma, Italy

<sup>f</sup> Dipartimento di Fisica dell'Università e Sezione INFN, Trieste, Italy

<sup>g</sup> Dipartimento di Fisica dell'Università "La Sapienza" e Sezione INFN, Roma, Italy

<sup>h</sup> Dipartimento di Fisica dell'Università e Sezione INFN, Lecce, Italy

<sup>i</sup> Dipartimento di Fisica dell'Università e Sezione INFN, Pisa, Italy

<sup>j</sup> Dipartimento di Fisica dell'Università e Sezione INFN, Bari, Italy

<sup>k</sup> Permanent address: Institute for High Energy Physics, CAS, Beijing, China

<sup>l</sup> Physics Department, State University of New York at Stony Brook, NY, USA

<sup>m</sup> Institut für Experimentelle Kernphysik, Universität Karlsruhe, Germany

<sup>n</sup> Dipartimento di Energetica dell'Università "La Sapienza", Roma, Italy

<sup>o</sup> Physics Department, University of Virginia, Charlottesville, VA, USA.

## 1 Introduction

The most recent measurement of  $R_S^\pi = \Gamma(K_S \rightarrow \pi^+\pi^-)/\Gamma(K_S \rightarrow \pi^0\pi^0)$  dates back to 1976. The authors quote an accuracy of 4.3% [1]. This and other results of similar accuracy determine the current world-average value of  $R_S^\pi$ ,  $2.197 \pm 0.026$ , the fractional error on which is 1.2%. Moreover, the averaging of the existing results is somewhat questionable, since the various experiments have not clearly described their procedures for handling radiative  $\pi^+\pi^-\gamma$  decays. It is currently of interest to improve the accuracy on  $R_S^\pi$ , with particular attention to an accurate determination of what part of the radiative spectrum is included in the quoted result [2]. The validity of the  $\Delta I = 1/2$  rule, empirically established in  $K$ ,  $\Lambda$ ,  $\Sigma$ , and  $\Xi$  decays, has never been satisfactorily understood. This lack of understanding is closely connected with the difficulty in relating  $\Re(\epsilon'/\epsilon)$  to the CKM matrix elements [3]. The value of  $R_S^\pi$  also enters into the theoretical calculation for the ratio of branching ratios for the decays  $K_L \rightarrow \mu^+\mu^-$  and  $K_L \rightarrow \pi^+\pi^-$  [4].

We describe the first measurement of  $R_S^\pi$  to achieve an accuracy below 1%, which moreover fully includes  $\pi^+\pi^-\gamma$  radiative decays. This should allow the extraction of the isospin  $I=0$  and  $I=2$  decay amplitudes.

The data were collected with the KLOE [5,6] detector at DAΦNE, the Frascati  $\phi$ -factory [7]. DAΦNE is an  $e^+e^-$  collider which operates at a center of mass energy of  $\sim 1020$  MeV, the mass of the  $\phi$ -meson. In the following, we use a coordinate system with the  $z$  axis along the nominal beam line, the  $x$  axis in the horizontal plane toward the machine center, the  $y$  axis vertical, and the origin at the center of the collision region. Equal-energy positron and electron beams collide at an angle of 25 mrad, producing  $\phi$ -mesons nearly at rest:  $p(\phi)_{y,z} = 0$  and  $p(\phi)_x = 12.5$  MeV/ $c$ .  $\phi$ -mesons decay  $\sim 34\%$  of the time into nearly collinear  $K^0\bar{K}^0$  pairs. Because  $J^{PC}(\phi) = 1^{--}$ , these pairs are in an antisymmetric state, so that the final state is always  $K_S K_L$ . Two photon intermediate states can lead to  $K_S K_S$  and  $K_L K_L$  final states, but this contamination is negligible [8,9]. All of the above implies that the detection of a  $K_L$  guarantees the presence of a  $K_S$  of given momentum and direction. This fact can be exploited to identify  $K_S$ -mesons independent of their decay mode. We refer to this technique as  *$K_S$  tagging*.

## 2 Experimental setup

The KLOE detector consists of a large cylindrical drift chamber, DC, surrounded by a lead-scintillating fiber sampling calorimeter, EMC. A superconducting coil surrounding the calorimeter provides a 0.52 T magnetic field.

The drift chamber [10], 4 m in diameter and 3.3 m long, has 12 582 all-stereo tung-

sten sense wires and 37 746 aluminum field wires. The chamber shell is made of carbon fiber-epoxy composite and the gas used is a 90% helium, 10% isobutane mixture. These features maximize transparency to photons and reduce  $K_L \rightarrow K_S$  regeneration and multiple scattering. The position resolutions are  $\sigma_{xy} \approx 150 \mu\text{m}$  and  $\sigma_z \approx 2 \text{ mm}$ . The momentum resolution is  $\sigma(p_\perp)/p_\perp \approx 0.4\%$ . Vertices are reconstructed with a spatial resolution of  $\approx 3 \text{ mm}$ .

The calorimeter [11] is divided into a barrel and two endcaps containing a total of 88 modules, and covers 98% of the solid angle. The modules are read out at both ends by photomultipliers. The arrival times of particles and the three-dimensional positions of the energy deposits are determined from the signals at the two ends. The readout granularity is  $\sim 4.4 \times 4.4 \text{ cm}^2$ ; the 2440 “cells” are arranged in layers five-deep. Cells close in time and space are grouped into a “calorimeter cluster.” For each cluster, the energy  $E_{\text{CL}}$  is the sum of the cell energies, and the time  $t_{\text{CL}}$  and position  $\vec{r}_{\text{CL}}$  are calculated as energy-weighted averages over the  $n$  cells. The energy and time resolutions are  $\sigma_E/E = 5.7\%/\sqrt{E(\text{GeV})}$  and  $\sigma_t = 54 \text{ ps}/\sqrt{E(\text{GeV})} \oplus 50 \text{ ps}$ , respectively.

While the trigger [12] uses calorimeter and chamber information, only the calorimeter trigger, which requires two local energy deposits above threshold (50 MeV on the barrel and 150 MeV on the endcaps), is used for the present measurement. Recognition and rejection of cosmic-ray events are also performed at the trigger level. Events with two energy deposits above a 30 MeV threshold in the outermost calorimeter plane are identified as cosmic-ray events and rejected. The trigger has a large time spread with respect to the beam crossing time. However, it is synchronized with the machine RF divided by 4,  $T_{\text{sync}} = 10.8 \text{ ns}$ , with an accuracy of 50 ps. The time  $T_0$  of the bunch crossing producing an event is determined after event reconstruction.

### 3 $K_S$ tagging

The mean decay lengths of the  $K_S$  and  $K_L$  are  $\lambda_S \sim 0.6 \text{ cm}$  and  $\lambda_L \sim 350 \text{ cm}$ . About 50% of  $K_L$ 's therefore reach the calorimeter before decaying. The  $K_L$  interaction in the calorimeter ( $K_L$ -crash) is identified by requiring a cluster of energy above 200 MeV, which is not associated with any track, and whose time corresponds to a velocity  $\beta = r_{\text{CL}}/ct_{\text{CL}}$  compatible with that of the  $K_L$ ,  $\beta(K_L) \sim 0.214$ . These  $K_L$ -crash events are used for  $K_S$  tagging. The tagging efficiency depends slightly on the  $K_S$  decay mode: the ratio  $R_{\text{tag}}$  of the tagging efficiencies for  $K_S \rightarrow \pi^+\pi^-$  and  $K_S \rightarrow \pi^0\pi^0$  is determined from data.

The interaction time  $T_0$ , which must be known for the measurement of the cluster times, is obtained from the first particle reaching the calorimeter (pions or photons for the

events of interest) assuming a velocity  $\beta = 1$ . In order to reduce the probability that  $T_0$  is accidentally determined from a particle arising from machine background, we require the  $T_0$  to be fixed by a cluster with energy  $E_{\text{CL}} > 50$  MeV and distance to the beam line  $\rho_{\text{CL}} > 60$  cm. Charged pions from  $K_S \rightarrow \pi^+\pi^-$  arrive at the EMC  $\sim 3$  ns later than  $\gamma$ 's from  $\pi^0$  decays. The computed time  $T_0$  is therefore delayed by one RF period,  $\sim 2.7$  ns. This results in a mismeasurement of the velocity for long-lived kaons accompanied by  $K_S \rightarrow \pi^+\pi^-$  decays. The distribution of the observed  $K_L$  velocity transformed to the  $\phi$ -rest frame,  $\beta^*$ , is shown in Fig. 1. The effect of the incorrect  $T_0$  assignment for the case of  $K_S \rightarrow \pi^+\pi^-$  is evident. Events are selected by requiring  $0.195 \leq \beta^* \leq 0.2475$ . This

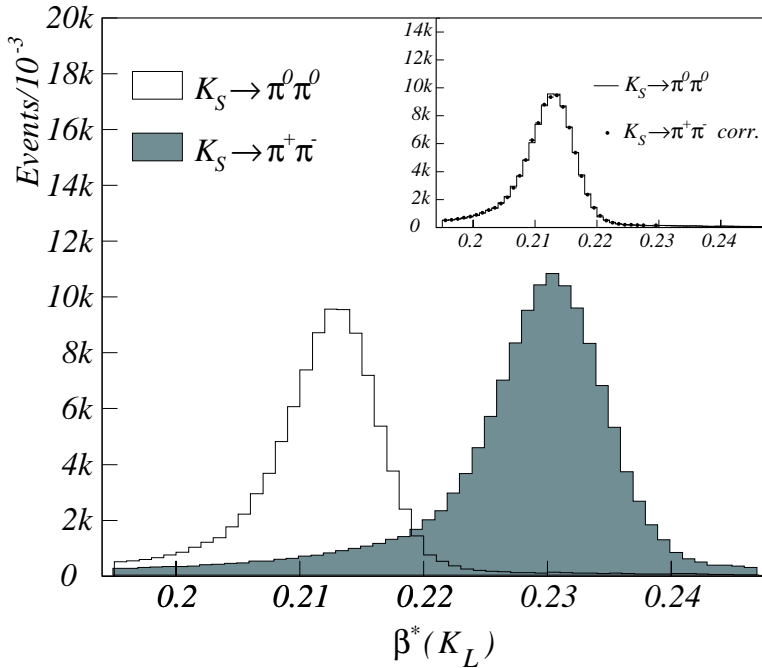


Figure 1: Distribution of the  $K_L$  velocity in the  $\phi$ -rest frame, for  $K_S \rightarrow \pi^0\pi^0$  (empty histogram) and  $K_S \rightarrow \pi^+\pi^-$  (shaded histogram) events. In the inset, the distribution for  $T_0$ -corrected  $K_S \rightarrow \pi^+\pi^-$  events (dots) is superimposed on that for  $K_S \rightarrow \pi^0\pi^0$  events (line).

window in  $\beta^*$  encompasses both peaks and gives a tagging efficiency of  $\sim 20\%$ , which differs slightly for each of the two  $K_S$  decay modes. The ratio of tagging efficiencies  $R_{\text{tag}}$  is evaluated from a subsample of  $K_S \rightarrow \pi^+\pi^-$  events in which both pion tracks are associated to a calorimeter cluster. In this case, the event  $T_0$  can be correctly evaluated making use of the measured pion track lengths and velocities, resulting in the  $\beta^*$  spectrum shown in the inset of Fig. 1, which is very similar to that for  $K_S \rightarrow \pi^0\pi^0$  events. This

corrected  $\beta^*$  distribution and that obtained from the standard  $T_0$  estimate are normalized to the same number of  $K_L$  interactions.  $R_{\text{tag}}$  is computed from the ratio of the total number of events inside the  $\beta^*$  window in each of the two cases. The effects of residual differences between the  $\beta^*$  distributions for  $K_S \rightarrow \pi^0\pi^0$  and  $T_0$ -corrected  $K_S \rightarrow \pi^+\pi^-$  events are included in the determination of the systematic error.

Other sources of bias in the evaluation of  $R_{\text{tag}}$  have been taken into account as well. The probability that the event contains a cluster which determines  $T_0$  is slightly different for  $\pi^+\pi^-$  and  $\pi^0\pi^0$  decays. These probabilities are estimated using  $K_S$  events tagged by  $K_L \rightarrow \pi^+\pi^-\pi^0$  decays. For the identification of such events, knowledge of  $T_0$  is not necessary. These events are identified by searching for two tracks forming a vertex in the drift chamber volume. The missing momentum of the  $\pi^0$  is determined by kinematic closure at the  $K_L$  vertex. Photons from the  $\pi^0$  are identified using *the difference* between their times of flight and by requiring that the  $\gamma\gamma$  pair be back-to-back in the  $\pi^0$  rest frame.

Accidental overlap of a  $\pi^\pm$  track with the  $K_L$  cluster produces a loss of  $K_S \rightarrow \pi^+\pi^-$  events. The magnitude of this effect has been estimated using  $K_L$ -crash events selected without requiring that the cluster not be associated with any track.

Finally, a small fraction of  $\phi \rightarrow K_S K_L$  events is rejected by the cosmic-ray veto, since some  $K_L$ -crash interactions can deposit energy in the outermost EMC plane.  $R_{\text{tag}}$  is therefore corrected by the ratio of the inefficiencies induced by the cosmic-ray veto for  $K_S \rightarrow \pi^+\pi^-$  and  $K_S \rightarrow \pi^0\pi^0$  events. This ratio is obtained using a subsample of events for which the cosmic-ray veto was recorded but not enforced.

All of the above effects result in corrections to  $R_{\text{tag}}$ , which are listed in Tab. 1. The largest uncertainty is due to the correction for the  $\beta^*$  cut.

#### 4 Selection of $K_S \rightarrow \pi^+\pi^-$ events

$K_S \rightarrow \pi^+\pi^-(\gamma)$  events are selected by requiring the presence of two tracks of opposite charge that intersect a cylinder 4 cm in radius and 10 cm in length along the  $z$ -axis, centered at the interaction region (IR). Pion momenta and polar angles must satisfy the fiducial cuts  $120 \leq p \leq 300 \text{ MeV}/c$  and  $30^\circ \leq \theta \leq 150^\circ$ . Pions must also reach the EMC, as opposed to spiralling in the drift chamber. The requirement that both tracks reach the EMC results in an acceptance which depends on the energy of the photon in radiative decays. Fig. 2 shows the dependence of the efficiency  $\epsilon_{\pi\pi\gamma}$  on the  $\gamma$  energy in the  $K_S$  rest frame  $E_\gamma^*$ , obtained by Monte Carlo (MC) simulation for  $K_S \rightarrow \pi^+\pi^-\gamma$  events with  $E_\gamma^* > 20 \text{ MeV}$  and  $K_S \rightarrow \pi^+\pi^-$  events without radiation ( $E_\gamma^* = 0$ ). The efficiency for  $0 < E_\gamma^* < 20 \text{ MeV}$  is obtained by linear interpolation. The overall acceptance is obtained by folding the above efficiency with the photon spectrum from Ref. [2]. The result differs

from that computed assuming no radiation by  $\sim 0.3\%$ .

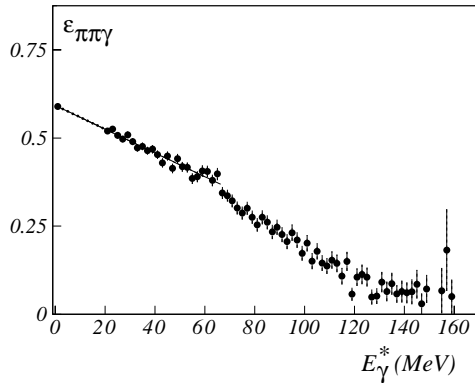


Figure 2: Efficiency for  $K_S \rightarrow \pi^+ \pi^- \gamma$  events vs radiated energy in the  $K_S$  rest frame  $E_\gamma^*$ , from Monte Carlo simulation.

The single-track reconstruction efficiency is obtained in bins of  $(p, \theta)$  using  $K_S \rightarrow \pi^+ \pi^-$  events identified by a single reconstructed pion track. This selection is applied to both data and MC. The ratio of data and MC reconstruction efficiencies is found to be constant ( $0.990 \pm 0.001$ ) for pions with momenta and polar angles that satisfy the fiducial cuts used in the analysis. The overall MC acceptance is therefore scaled accordingly and used to correct the data. Systematic errors due to possible misalignments of the DC are evaluated by studying the dependence of the acceptance on the angular cut applied and are found to be negligible. The acceptance is listed in Tab. 1.

The trigger efficiency is also obtained from data.  $K_L$  interactions always fire at least one trigger sector. About 40% of the time, however, the  $K_L$ -crash fires two nearby sectors, thus producing a valid trigger by itself. We use these events to find the probability that at least one  $K_S$  decay product complements the  $K_L$ -crash cluster to satisfy the trigger condition in the remaining 60% of the events. The trigger efficiency is given in Tab. 1.

## 5 Selection of $K_S \rightarrow \pi^0 \pi^0$ events

$K_S \rightarrow \pi^0 \pi^0$  events are identified by the prompt photon clusters from  $\pi^0$  decays. A prompt photon cluster must satisfy  $|t_{\text{CL}} - r_{\text{CL}}/c| \leq 5\sigma_t$ , where  $\sigma_t$  is the energy-dependent time resolution, and must not be associable to any track. Machine background is reduced by cuts on energy and polar angle; we require  $E_{\text{CL}} > 20$  MeV and  $\cos \theta < 0.9$ . Three or more prompt photons are required to accept a  $K_S \rightarrow \pi^0 \pi^0$  event.

The photon-detection efficiency in bins of energy and polar angle has been obtained from data using a sample of  $\phi \rightarrow \pi^+ \pi^- \pi^0$  events. The acceptance for  $K_S \rightarrow \pi^0 \pi^0$  events

is obtained from MC simulation and is listed in Tab. 1. The simulation incorporates the experimentally determined photon-detection efficiencies; we rely on it essentially for the averaging over event geometries and kinematics. The 0.2% error on the  $K_S \rightarrow \pi^0\pi^0$  selection efficiency is dominated by the uncertainty in the photon-detection efficiency below 50 MeV due to non-linearity in the energy response of the calorimeter and/or the photon reconstruction algorithm. The trigger efficiency, also listed in Tab. 1, is evaluated by the same method used for  $K_S \rightarrow \pi^+\pi^-$  events.

Background in the sample of  $K_S \rightarrow \pi^0\pi^0$  events is mainly due to  $K_S \rightarrow \pi^+\pi^-$  events in which the track-to-cluster association failed, and in which there were residual split and accidental clusters. This contamination induces an error on the counting of events with three or more prompt clusters that is lower than 0.1%, as estimated directly from data.

Source	$R_{\text{tag}}$
$\beta^*$ window	$0.986 \pm 0.005$
$T_0$ efficiency	$0.990 \pm 0.001$
Track-cluster association	$0.998 \pm 0.002$
Cosmic-ray veto	$1.003 \pm 0.002$
Total	$0.977 \pm 0.005$
	$\epsilon(\pi^+\pi^-)$
Event selection	$0.5760 \pm 0.0015$
Trigger	$0.989 \pm 0.001$
Total	$0.5697 \pm 0.0016$
	$\epsilon(\pi^0\pi^0)$
Event selection	$0.9005 \pm 0.0018$
Trigger	$0.9986 \pm 0.0004$
Total	$0.8992 \pm 0.0018$

Table 1: The analysis steps are listed, together with the associated efficiencies.

## 6 Result

The present measurement of  $R_S^\pi$  is based on an integrated luminosity of  $17 \text{ pb}^{-1}$  collected during the year 2000. The data set contains  $N^\pm = 1\,060\,821$  selected  $K_S \rightarrow \pi^+\pi^-$  events and  $N^{00} = 766\,308$  selected  $K_S \rightarrow \pi^0\pi^0$  events. The value for  $R_S^\pi$  is obtained by correcting the ratio of these numbers for the ratio of tagging and selection (including trigger)



efficiencies:

$$R_S^\pi = \frac{N^\pm}{N^{00}} \times \frac{1}{R_{\text{tag}}} \times \frac{\epsilon_{\text{sele}}^{00}}{\epsilon_{\text{sele}}^\pm}$$

The result is

$$2.236 \pm 0.003_{\text{stat}} \pm 0.015_{\text{syst}}$$

The contributions to the estimated errors are listed in Tab. 2. Additional details are available in Ref. [13]. Our result is consistent with but slightly higher than the current world-average value  $R_S^\pi = 2.197 \pm 0.026$  [14]. This might be expected, since our measurement was designed to include the entire radiative spectrum.

Source	Error, %
Event count	0.14
Tracking	0.26
Cluster counting	0.20
Trigger	0.10
Ratio of tag efficiencies	0.55
Cosmic-ray veto	0.21
Total error	0.70

Table 2: Contributions to the fractional error on  $R_S^\pi$ .

## 7 Acknowledgments

We thank the DAΦNE team for their efforts in maintaining low background running conditions and their collaboration during all data-taking. We also thank F. Fortugno for his efforts in ensuring good operations of the KLOE computing facilities. This work was supported in part by DOE grant DE-FG-02-97ER41027; by EURODAPHNE contract FMRX-CT98-0169; by the German Federal Ministry of Education and Research (BMBF) contract 06-KA-957; by Graduiertenkolleg 'H.E. Phys. and Part. Astrophys.' of Deutsche Forschungsgemeinschaft contract No. GK 742; by INTAS contracts 96-624 and 99-37; and by TARI contract HPRI-CT-1999-00088.

## References

- [1] G. Everhart, et al., Phys. Rev. D14 (1976) 661–666.
- [2] V. Cirigliano, J. F. Donoghue, E. Golowich, Eur. Phys. J. C18 (2000) 83–95.

- [3] M. Ciuchini, G. Martinelli, Nucl. Phys. Proc. Suppl. 99B (2001) 27–34.
- [4] L. Littenberg, to appear in the Proceedings of 9th International Symposium on Heavy Flavor Physics, Pasadena, CA, 10-13 Sep 2001. (2002).  
URL <http://www.arXiv.org/ps/hep-ex/0201026>
- [5] KLOE collaboration, M. Adinol£, *et al.*, KLOE: A general purpose detector for DAΦNE, LNF-92/019 (IR).
- [6] KLOE collaboration, M. Adinol£, *et al.*, The KLOE detector, technical proposal, LNF-93/002 (IR).
- [7] S. Guiducci, Status of DAΦNE, in: P. Lucas, S. Webber (Eds.), Proc. of the 2001 Particle Accelerator Conference - Chicago, IL U.S.A., 2001, p. 353.
- [8] I. Dunietz, J. Hauser, J. Rosner, Phys. Rev. D35 (1987) 2166.
- [9] N. Brown, F. E. Close, Scalar mesons and kaons in  $\phi$  radiative decay & their implications for studies of CP violation at DAΦNE, in: L. Maiani, G. Pancheri, N. Paver (Eds.), The DAΦNE Physics Handbook, Vol. 2, 1992, p. 447.
- [10] KLOE collaboration, M. Adinol£, *et al.*, Nucl. Inst. Meth. A, in press.
- [11] KLOE collaboration, M. Adinol£, *et al.*, Nucl. Inst. Meth. A482 (2002) 363.
- [12] KLOE collaboration, M. Adinol£, *et al.*, The KLOE trigger system, LNF Report LNF-02/02 (P), submitted to Nucl. Inst. Meth.
- [13] M. Palutan, T. Spadaro, P. Valente, Measurement of  $\Gamma(K_S \rightarrow \pi^+ \pi^- (\gamma)) / \Gamma(K_S \rightarrow \pi^0 \pi^0)$  with KLOE 2000 data, KLOE note 174 (2002).  
URL <http://www.lnf.infn.it/kloe/pub/knote/kn174.ps.gz>
- [14] D. E. Groom, *et al.*, Eur. Phys. J. C15 (2000) 1.